CrossMark

Effect of SiO$_2$ on optical properties of bismuth-doped B$_2$O$_3$–GeO$_2$–SiO$_2$ glasses

Zhousu Xu[1] · Jinhua Yan[1] · Cheng Xu[2] · Hang Zhang[1] · Gang Chen[1] · Xiaofeng Liu[2] · Jianrong Qiu[3]

Abstract

Bi-doped (60-x)GeO$_2$–xSiO$_2$–15B$_2$O$_3$–20MgO–5Al$_2$O$_3$–0.5Bi$_2$O$_3$ (x = 0, 5, 10, 15,20, 25 mol%)glasses were prepared by a conventional melt-quenching process. A broad near-infrared (NIR) photoluminescence (PL) band from Bi centers centered around 1100 nm with a large full-width-at-half-maximum value (~ 195 nm) was observed under excitation at 700 nm. Along with the increase of SiO$_2$ concentration, the NIR PL intensity and the quantum yield (44.1–51.2%) increase first and then decrease, and the PL lifetime increases from 409 to 464 μs. The spectroscopic properties can be interpreted in terms of Bi centers with different valence states, which were confirmed by two-dimension photoluminescence excitation map spectra. The dependence of optical properties on SiO$_2$ concentration is mainly attributed to the change of the optical basicity among different samples. This Bi-doped B$_2$O$_3$–GeO$_2$–SiO$_2$ glass could find potential application in fiber amplifier and laser due to the efficient and tunable broad NIR luminescence.

1 Introduction

Recently, Bi-doped glasses have attracted growing attention because of their long photoluminescence (PL) lifetime and broadband near-infrared (NIR) emission. Since Fujimoto et al. [1]reported that Bi-doped silica glass exhibited strong NIR emission with large full-width-at-half-maximum (FWHM), various glass systems doped with Bi using the melt-quenching method have been reported, such as silicate [1–4], borate [5, 6], germanate [7–9], oxyfluoride [10], phosphate [11–13], and chalcohalide [14, 15] glasses. Due to their unique optical properties, Bi-doped glasses are

regarded to have potential application in various photoelectric devices, such as fiber lasers and fiber amplifiers [16]. In 2005, Dianov et al. [17] proposed and fabricated the first continuous wave laser in the spectral region between 1150 and 1300 nm using a Bi-doped aluminosilicate glass fiber, which is a milestone in the development of Bi-doped glasses and relevant photoelectric devices. In 2016, Thipparapu et al. [18] reported a high gain (~ 25 dB) Bi-doped fiber amplifier operating in the wavelength band 1320–1360 nm.

For Bi-doped glasses, the topological network structure of glass plays an important role in various spectroscopic properties of Bi ions. Mixed network effect on the NIR emission of Bi centers has been reported in different oxide glass systems, such as borogermanate [19, 20], borosilicate [21, 22], phosphosilicate [23], and germanosilicate [24, 25] glasses. In these glasses, it is generally considered that the Bi ion with low valence states (possibly Bi$^+$) contribute to the NIR emission, and the phonon energy and the optical basicity have strong effect on the PL behavior of Bi-doped glasses. Apart from the spectroscopic results, the quantum yield (QY) of Bi-doped glass and a possible means for modulating the PL lifetime have rarely been reported for glass system, although these are believed to be very important parameters for photoelectric devices. Therefore, it is of significance to investigate the effect of glass topological network structure on the QY and PL lifetime of Bi-doped B$_2$O$_3$–GeO$_2$–SiO$_2$ glasses.

✉ Xiaofeng Liu
xfliu@zju.edu.cn

✉ Jianrong Qiu
qjr@zju.edu.cn

1 Institute of Intelligent Optoelectronic Technology, Zhejiang University of Technology, Hangzhou 310014, China

2 School of Materials Science and Engineering, Zhejiang University, Hangzhou 310027, China

3 State Key Laboratory of Modern Optical Instrumentation, College of Optical Science and Engineering, Zhejiang University, Hangzhou 310027, China

In this investigation, SiO_2 was introduced into Bi-doped GeO_2–SiO_2–B_2O_3–MgO–Al_2O_3 glasses aiming to modulate the NIR emission of Bi centers. It is found that the NIR PL intensity and the QY increase first and then decrease, while the PL lifetime increases with increasing SiO_2 concentration. Furthermore, the change of the glass network structure was confirmed by a Fourier transform infrared (FT-IR) spectrometer. The results indicate that the network structure strongly affects the PL behavior, such as the PL intensity, the QY and the PL lifetime.

2 Experimental

The glass samples with compositions (in mol%) of (60-x) GeO_2–$x$$SiO_2$–$15B_2O_3$–$20MgO$–$5Al_2O_3$–$0.5Bi_2O_3$ (x=0, 5, 10, 15, 20, 25 mol%, denoted as GSBx) were prepared by the conventional melt-quenching method. The raw materials are analytical grade pure SiO_2, H_3BO_3, MgO, Al_2O_3, Bi_2O_3, and 5N (99.999%) GeO_2. In a typical procedure, 20 g powder mixtures were mixed thoroughly in an agate mortar, and then melted in an alumina crucible at 1550 °C for 40 min in air. Afterwards, the melt was quenched onto a stainless steel plate and pressed with another stainless steel plate. The samples were then cut and polished for optical measurements.

Optical absorption spectra were recorded with a UV-3600 UV–Vis-NIR spectrophotometer (Shimadzu Instruments, Kyoto, Japan). The emission spectra, two-dimension (2D) photoluminescence excitation (PLE) map spectra and fluorescent decay kinetics were measured with a FLS 980 fluorescence spectrometer (Edinburgh Instruments, Livingston, UK) equipped with a Xe lamp and μs flash Xe lamp as the excitation source. The glass network was characterized by FT-IR spectra with a Nicolet 6700 spectrometer (Thermo Fisher Scientific Inc., Waltham, MA, USA). The QY was measured with an absolute photoluminescence quantum yield measurement system (Quantaurus-QY Plus C13534-35, Hamamatsu Corp., Shizuoka, Japan). All the measurements were carried out at room temperature.

3 Results and discussion

The obtained glasses are brownish red, as shown in the inset of Fig. 1. From the absorption spectra of the glass samples shown in Fig. 1, two characteristic absorption bands centering at about 500 and 700 nm could be clearly observed, which are similar to the characteristic Bi-related absorption bands observed in different glasses [5, 19, 20]. The absorption band centering at about 500 nm can be ascribed to Bi^{+}: $^3P_0 \rightarrow {}^1D_2$ and Bi^{0}: $^4S_{3/2} \rightarrow {}^2P_{1/2}$, while the band centering at about 700 nm can be attributed to $^3P_0 \rightarrow {}^3P_2$ transition of Bi^+ [25]. The dependencies of absorption intensity
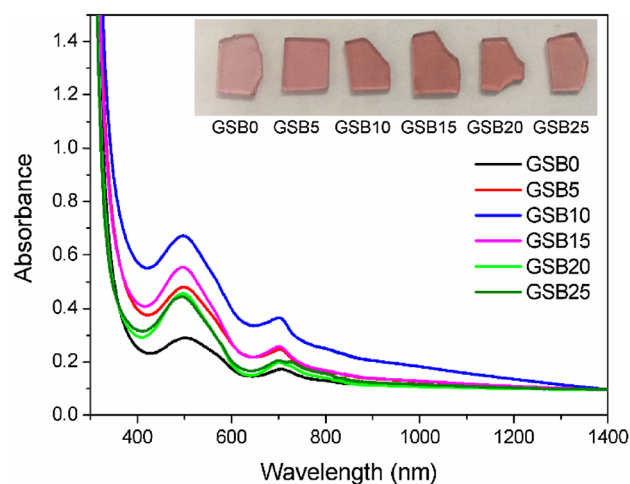

Fig. 1 Optical absorption spectra of the glass samples. The inset is the photographs of the glass samples

at 700 nm on SiO_2 concentration are shown in Fig. 2b. The absorption intensity in Fig. 2b is the integrated intensity of the absorption band derived from Bi centers after subtracting the contribution of baseline. The result shows a clear dependence of the absorption of the Bi centers on the glass composition.

Figure 2a shows the NIR PL spectra of the glass samples under excitation at 700 nm with different SiO_2 concentrations. A broadband PL at about 1100 nm with a FWHM value of 195 nm is observed in the glass samples. The NIR emission is generally attributed to Bi ions with low valence states, such as Bi^+. It is found that the NIR PL intensity increases first, and then decreases with the rise of SiO_2 concentration, as shown in Fig. 2b, which is similar to the change of absorption intensity. Both absorption and PL reach maximum intensities for the sample with 10% SiO_2 (GSB10). With increasing SiO_2 concentration, the peak PL wavelength undergoes a tiny red shift, which can be attributed to the change of glass composition. Along with the increase of SiO_2 concentration, the PL intensity under excitation at 500 nm also shows the same trend, which is shown in the Table 2 and the Supplementary Fig. 1.

Figure 2c, d show the visible PL spectra of the glass samples under excitation at 320 and 475 nm. A blue emission band centered at 420 nm under 320 nm excitation can be ascribed to Bi^{3+}: $^3P_1 \rightarrow {}^1S_0$ [10]. With the rise of SiO_2 concentration, its intensity decreases first, and then increases, as shown in Fig. 2c. In comparison, the red emission due to the Bi^{2+}: $^2P_{3/2} \rightarrow {}^2P_{1/2}$ transition centered at 655 nm (excited at 470 nm) increases with the rise of SiO_2 concentration from 0 to 25%, as shown in Fig. 2d.

To understand the NIR luminescence of the Bi centers, we performed 2D-PLE map spectroscopy measurement to locate the excitation energies corresponding to distinct
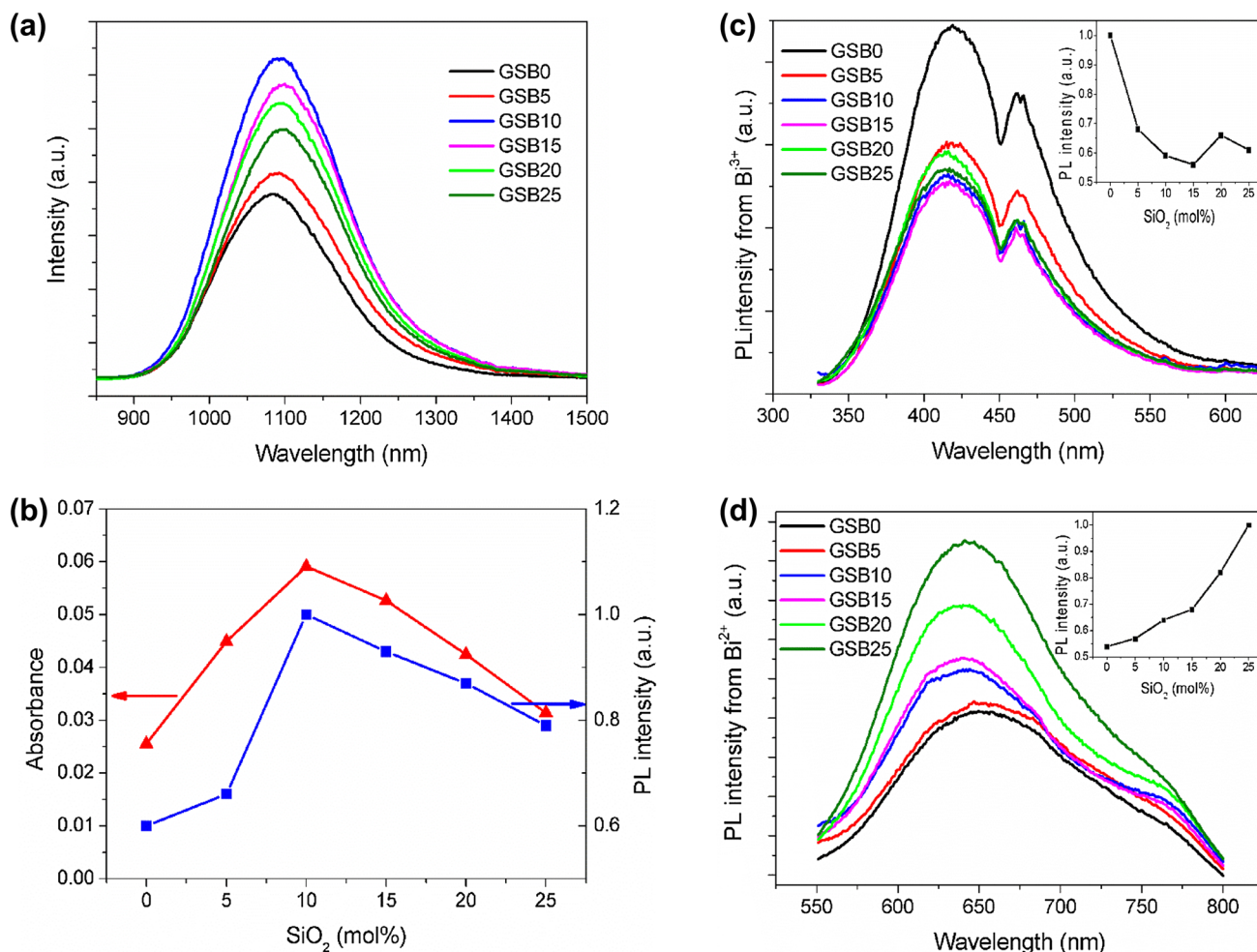
Fig. 2 a Emission spectra of the glass samples in the NIR region under excitation at 700 nm. **b** Dependence of NIR emission intensity and absorbance at 700 nm on the SiO₂ concentration. **c, d** Emission spectra of the glass samples in the visible region under excitation at 320 and 470 nm. The inset is the dependence of PL intensity on the SiO₂ concentration

energy levels. Figure 3 shows the normalized 2D-PLE contour maps for glass samples GSB0, GSB10 and GSB25, which indicate that the position of the emission peak strongly depends on the excitation wavelength. The glass samples exhibit three distinct peaks, indicating there are multiple Bi-related excitation and emission centers. Three excitation bands were observed at around 330, 510 and 700 nm, and the corresponding emission bands were located at around 1100 nm. Because the PL intensity with emission wavelength at around 1250 nm was relatively small, the emission band at around 1250 nm was absent in 2D-PLE contour maps. To further analyze the Bi-related optical centers, the contour map was divided into three areas (denoted as 1, 2, 3), and the peak intensity of corresponding area was denoted as I_1, I_2 and I_3, respectively, as shown in Fig. 3a. This allows the calculation of the intensity ratios (I_2/I_1 and I_3/I_1) for the glass samples GSB0, GSB10 and GSB 25, as shown in Table 1. The results show that the value of I_2/I_1 is

almost unchanged, but the value of I_3/I_1 decreases obviously with the increase of SiO₂ concentration. The result suggests that the excitation peak located at around 510 and 700 nm may be attributed to the same Bi centers, and the excitation peak located at around 330 nm should be attributed to another Bi center of a different valence state, which decreases in concentration with the increase in SiO₂ concentration.

To understand the change of the PL intensity by SiO₂ addition in the glasses, we recorded the fluorescent decay curves at 1100 nm for the glass samples under excitation at 700 nm, as shown in Fig. 4. By fitting the decay curves with the single exponential decay function, the derived PL lifetime of bismuth-doped B₂O₃–GeO₂–SiO₂ glasses under excitation at 700 nm increases from 409 to 464 μs with the increase of SiO₂ concentration, as listed in Table 2. The PL lifetime under excitation at 500 nm shows the same trend with the increase of SiO₂ concentration, which is shown in the Table 2 and the Supplementary Fig. 2. Whereas the
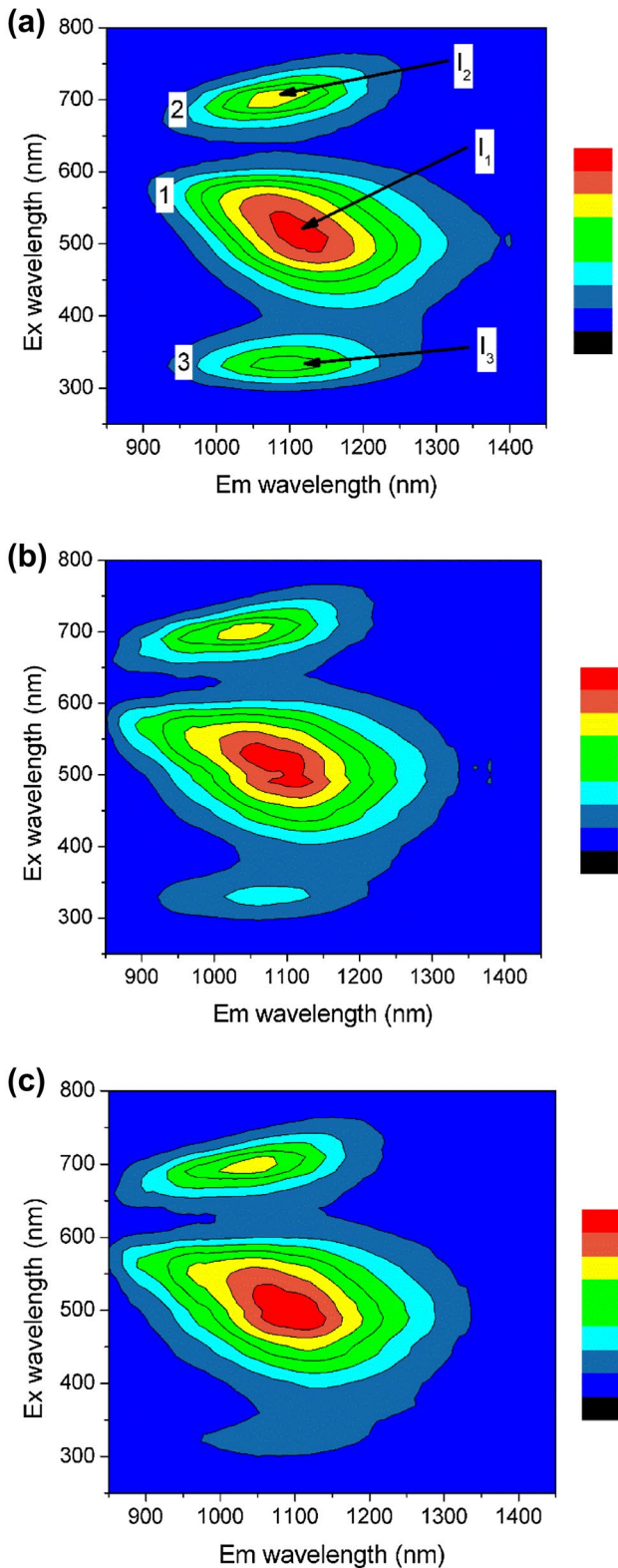
Fig. 3 Normalized 2D PLE maps of glass samples. **a** GSB0, **b** GSB10, **c** GSB25

Table 1 The calculated intensity ratio of different samples

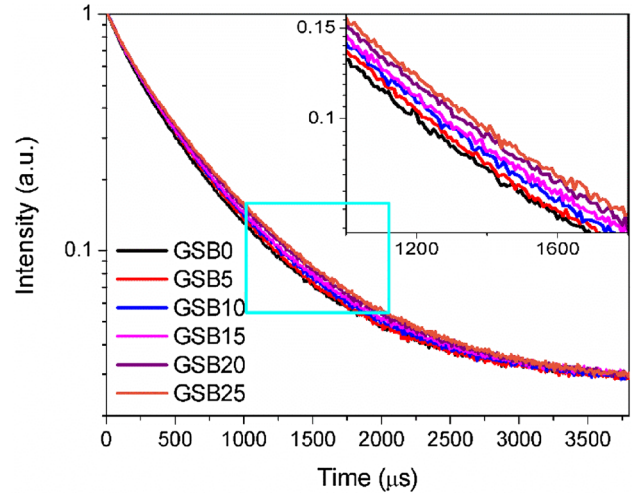| Sample	GSB0	GSB10	GSB25
I_2/I_1	0.76	0.76	0.75
I_3/I_1	0.61	0.32	0.21

Fig. 4 Fluorescent decay curves of the glass samples recorded at the excitation wavelength of 700 nm. The inset is a magnified figure of the area within the light blue square frame

phonon energy of the glass may have changed with the increase in SiO_2 concentration, the increase of PL lifetime may be attributed to the decrease of radiative transition rate. According to Fermi's golden rule, the radiative decay rate in a homogeneous dielectric medium (Γ_r) can be calculated by the equation below [26],
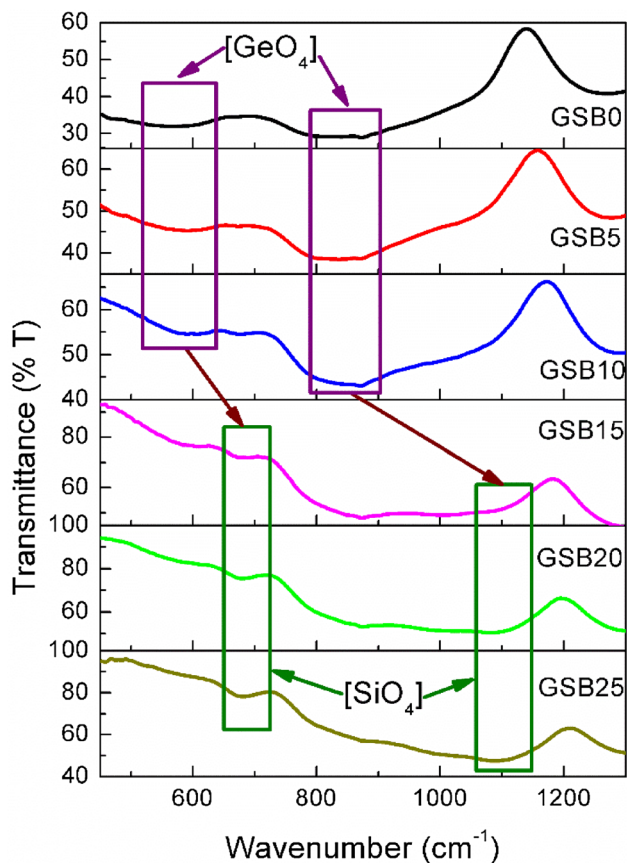
$$\Gamma_r = n\Gamma_0, \tag{1}$$

where n is medium refractive index, Γ_0 is radiative decay rate in vacuum. For the Bi-doped B_2O_3–GeO_2–SiO_2 glasses studied here, the increase in the concentration of SiO_2 leads to the reduction in refractive index and thus decrease of the radiative process. A similar dependence of transition rate on the dielectric constant of the host have been observed in RE-doped oxide glass as well as in RE-doped nanocrystals dispersed in solvents [26, 27].

The QY was measured under excitation at 500 and 700 nm. It is found that the QY increases first, and then decreases with the rise of SiO_2 concentration, as shown in Table 2, which is similar to the change of PL intensity.

To understand the PL behavior and its dependence on the glass composition, we recorded FT-IR spectra for the glass samples. Figure 5 shows the FT-IR spectra of the glass samples, where four main absorption bands could be observed. The absorption bands located at around 580 and 873 cm^{-1} are attributed to the Ge–O symmetric and

Table 2 Spectroscopic properties of Bi-doped glass samples under excitation at 500 and 700 nm

| λ_{ex} (nm)	Samples	GSB0	GSB5	GSB10	GSB15	GSB20	GSB25
700	Normalized PL intensity	0.60	0.66	1.00	0.93	0.87	0.79
	PL lifetime (μs)	409	423	430	435	452	464
	QY (%)	44.1	44.8	51.2	48.4	47.8	47.7
500	Normalized PL intensity	0.61	0.68	1.00	0.89	0.81	0.73
	PL lifetime (μs)	263	282	283	285	296	303
	QY (%)	42.1	42.7	47.0	45.4	44.6	41.8

Fig. 5 FT-IR spectra of glass samples

asymmetric stretching vibration of [GeO$_4$] tetrahedron unit, respectively [28, 29]. The absorption bands located at around 680 and 1070 cm^{-1} are ascribed to Si–O symmetric and asymmetric stretching vibration of [SiO$_4$] tetrahedron unit, respectively [30–32]. The results show that this glass network mainly consists of [SiO$_4$] and [GeO$_4$] tetrahedron units through interconnection of apical oxygen atoms. It is also found that the intensity of [GeO$_4$] tetrahedron unit at 580 and 873 cm^{-1} decreases and the intensity of [SiO$_4$] tetrahedron unit at 680 and 1070 cm^{-1} increases with increasing SiO$_2$ concentration (Fig. 5), indicating the growth in the number of [SiO$_4$] tetrahedron unit.

Usually, Bi ions with different oxidation states or Bi clusters coexist in oxide glasses. Recently, Bi ions with low oxidation states such as Bi$^+$ and Bi^0 have been regarded as the origin of NIR emission [10, 22, 25]. According to the optical basicity theory proposed by Duffy [33, 34], metal species tend to stabilize at their low oxidation state in the glasses with lower optical basicity. It has been reported previously that low optical basicity favors Bi ions with low oxidation states (such as Bi$^+$, Bi^0) [10, 35, 36]. The optical basicity (Λ) of glasses can be calculated using the Eq. (2):

$$\Lambda = X_1\Lambda_1 + X_2\Lambda_2 + \cdots + X_n\Lambda_n, \tag{2}$$

where X_n is equivalent fractions based on the amount of oxygen contributing to the overall glass stoichiometry, and Λ_n is the optical basicity of the oxide. The optical basicity of silicate glass (0.48–0.52) is smaller than that of the germanate glass (0.60–0.94). It is apparent that the optical basicity of the oxide glasses is expected to decrease with the increase in SiO$_2$ concentration, which favors the following process:

Bi^{3+} → Bi^{2+} → Bi$^+$ → Bi^0.
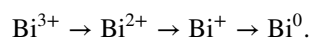
Furthermore, according to Fig. 2b, the absorption intensity centering at about 700 nm increases first, and then decreases with the rise of SiO$_2$ concentration. The absorption reaches maximum intensity for the sample with 10% SiO$_2$ (GSB10). The absorption band at about 700 nm is attributed to $^3P_0 \rightarrow {}^3P_2$ transition of Bi$^+$ [25], as shown in Fig. 6, which indicates the concentration of Bi$^+$ ions increases with increasing SiO$_2$ concentration from 0 to 10 mol%, and then decreases because of reduction to Bi^0 with further increase of SiO$_2$ concentration. The NIR emission centered at approximately 1100 nm is attributed to $^3P_1 \rightarrow {}^3P_0$ transition of Bi$^+$ [25], as shown in Fig. 6. Therefore, the NIR PL intensity increases first, and then decreases with the rise of SiO$_2$ concentration, which is in line with the change of Bi$^+$ ion concentration.

In addition, the maximum phonon energy of silicate glass is higher than that of the germanate glass. Therefore, the electron–phonon coupling strength in the Bi-doped B$_2$O$_3$–GeO$_2$–SiO$_2$ glasses are expected to increase with the increase in SiO$_2$ concentration, which can increase the probability of phonon-assisted nonradiative process and thus decrease the PL intensity. Compared with the effect of Bi$^+$
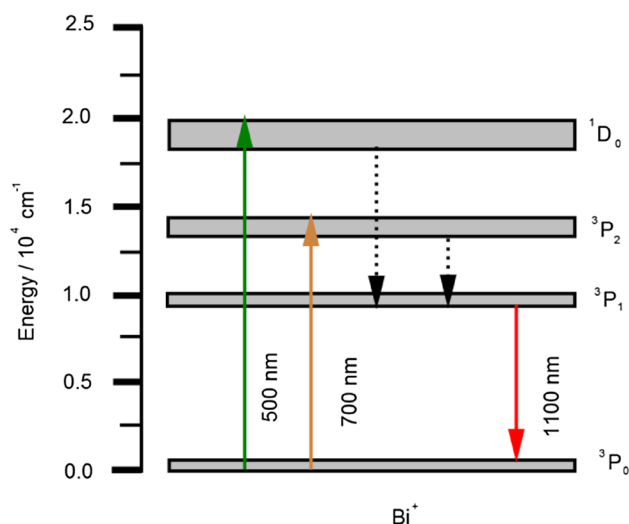
Fig. 6 Energy level scheme of Bi^+

ion concentration, the effect of phonon energy on NIR PL is small, considering the fact that each component in a multi-component glass contribute to the vibrational properties. Therefore, we mainly consider here the influence of Bi^+ ion concentration on the NIR PL intensity.

4 Conclusions

Bismuth-doped GeO_2–SiO_2–B_2O_3–MgO–Al_2O_3 glasses were prepared by the conventional high-temperature melt-quenching method. The Bi-doped B_2O_3–GeO_2–SiO_2 glasses shows a broad NIR emission band with large FWHM value (~ 195 nm), and the position of the emission peak strongly depends on the excitation wavelength. With the increase in SiO_2 concentration, the NIR PL intensity increases first, and then decreases. The NIR PL lifetime under excitation at 700 nm increases from 409 to 464 μs and the QY under excitation at 700 nm is found to be in the range of approximately 44.1–51.2% with the rise of SiO_2 concentration. The 2D-PLE map indicates the NIR emission from multiple Bi centers may involve multiple energy states. The evolution of optical properties is mainly attributed to the change in optical basicity and the oxidation state of Bi centers resulted from the rise of SiO_2 concentration. The large FWHM and strong NIR emission of Bi-doped B_2O_3–GeO_2–SiO_2 glass may facilitate its application in NIR optical amplifiers and lasers.

References

1. Y. Fujimoto, M. Nakatsuka, Infrared luminescence from bismuth-doped silica glass. Jpn. J. Appl. Phys. **40**(3B), 279–281 (2001)
2. S.F. Zhou, N. Jiang, B. Zhu, H. Yang, S. Ye, G. Lakshminarayana, J. Hao, J.R. Qiu, Multifunctional bismuth-doped nanoporous silica glass: from blue-green, orange, red, and white light sources to ultra-broadband infrared amplifiers. Adv. Funct. Mater. **18**(9), 1407–1413 (2008)
3. P.S. Yu, L.B. Su, W. Guo, J. Xu, Broadband infrared luminescence in Bi-doped silicate glass. J. Noncryst. Solids **464**, 34–38 (2017)
4. B. Denker, B. Galagan, V. Osiko, I. Shulman, S. Sverchkov, E. Dianov, Absorption and emission properties of Bi-doped Mg–Al–Si oxide glass system. Appl. Phys. B **95**(4), 801–805 (2009)
5. X.G. Meng, J.R. Qiu, M.Y. Peng, D.P. Chen, Q.Z. Zhao, X.W. Jiang, C.S. Zhu, Infrared broadband emission of bismuth-doped barium-aluminum-borate glasses. Opt. Express **13**(5), 1635–1642 (2005)
6. Q.B. Guo, B.B. Xu, D.Z. Tan, J.C. Wang, S.H. Zheng, W. Jiang, J.R. Qiu, S.F. Zhou, Regulation of structure rigidity for improvement of the thermal stability of near-infrared luminescence in Bi-doped borate glasses. Opt. Express **21**(23), 27835–27840 (2013)
7. M.Y. Peng, J.R. Qiu, D.P. Chen, X.G. Meng, I. Yang, X.W. Jiang, C.S. Zhu, Bismuth- and aluminum-codoped germanium oxide glasses for super-broadband optical amplification. Opt. Lett. **29**(17), 1998–2000 (2004)
8. R.F. Wang, J. Liu, Z. Zhang, Luminescence and energy transfer progress in Bi-Yb co-doped germanate glass. J. Alloys Compd. **688**, 332–336 (2016)
9. M.Y. Peng, X.G. Meng, J.R. Qiu, Q.Z. Zhao, C.S. Zhu, GeO_2: Bi, M (M = Ga, B) glasses with super-wide infrared luminescence. Chem. Phys. Lett. **403**(4–6), 410–414 (2005)
10. B.B. Xu, D.Z. Tan, S.F. Zhou, Z.L. Hong, K.N. Sharafudeen, J.R. Qiu, Enhanced broadband near-infrared luminescence of Bi-doped oxyfluoride glasses. Opt. Express **20**(27), 29105–29111 (2012)
11. A. Moguš-Milanković, A. Šantić, V. Ličina, D.E. Day, Dielectric behavior and impedance spectroscopy of bismuth iron phosphate glasses. J. Noncryst. Solids **351**(40–42), 3235–3245 (2005)
12. J. Ruan, E. Wu, H.P. Zeng, S.F. Zhou, G. Lakshminarayana, J.R. Qiu, Enhanced broadband near-infrared luminescence and optical amplification in Yb-Bi codoped phosphate glasses. Appl. Phys. Lett. **92**(10), 1011213 (2008)
13. B. Denker, B. Galagan, V. Osiko, S. Sverchkov, E. Dianov, Luminescent properties of Bi-doped boro-alumino-phosphate glasses. Appl. Phys. B **87**(1), 135–137 (2007)
14. Q.Q. Yan, C. Shen, W. Wang, S.F. Wang, G.R. Chen, Z.W. Xing, Near infrared emission and energy transfer of bismuth–thulium co-doped chalcohalide glasses. J. Am. Ceram. Soc. **93**(11), 3539–3541 (2010)
15. G. Yang, D.P. Chen, W. Wang, Y.S. Xu, H.D. Zeng, Y.X. Yang, G.R. Chen, Effects of thermal treatment on broadband near-infrared emission from Bi-doped chalcohalide glasses. J. Eur. Ceram. Soc. **28**(16), 3189–3191 (2008)
16. J.R. Qiu, Bi-doped glass for photonic devices. Int. J. Appl. Glass Sci. **6**(3), 275–286 (2015)
17. E.M. Dianov, V.V. Dvoyrin, V.M. Mashinsky, A.A. Umnikov, M.V. Yashkov, A.N. Guryanov, CW bismuth fibre laser. Quantum Electron. **35**(12), 1083–1084 (2005)
18. N.K. Thipparapu, A. Umnikov, P. Barua, J.K. Sahu, Bi-doped fiber amplifier with a flat gain of 25 dB operating in the wavelength band 1320–1360 nm. Opt. lett. **41**(7), 1518–1521 (2016)
19. N. Zhang, K.N. Sharafudeen, G.P. Dong, M.Y. Peng, J.R. Qiu, Mixed network effect of broadband near-infrared emission in Bi-doped B_2O_3–GeO_2 glasses. J. Am. Ceram. Soc. **95**(12), 3842–3846 (2012)

20. Z.S. Xu, C. Xu, Q.B. Guo, X.F. Liu, J.R. Qiu, Effect of TeO₂ on near-infrared emission from bismuth centers in borogermanate glasses. J. Am. Ceram. Soc. **99**(3), 760–764 (2016)

21. R.H. Wan, Z.G. Song, Y.J. Li, Y.T. Zhou, Q. Liu, J.B. Qiu, Z.W. Yang, Z.Y. Yin, Investigation on the near-infrared-emitting thermal stability of Bi activated alkaline-earth aluminoborosilicate glasses. J. Appl. Phys. **117**(5), 053107 (2015)

22. S.F. Zhou, Q.B. Guo, H. Inoue, Q. Ye, A. Masuno, B.B. Zheng, Y.Z. Yu, J.R. Qiu, Topological engineering of glass for modulating chemical state of dopants. Adv. Mater. **26**(47), 7966–7972 (2014)

23. Z.G. Song, Z.W. Yang, D.C. Zhou, Z.Y. Yin, C. Li, R.F. Wang, J.H. Shang, K. Lou, Y.Y. Xu, X. Yu, J.B. Qiu, The effect of P₂O₅ on the ultra-broadband near-infrared luminescence from bismuth-doped SiO₂–Al₂O₃–CaO glass. J. Lumin. **131**(12), 2593–2596 (2011)

24. B.I. Denker, S.V. Firstov, B.I. Galagan, S.E. Sverchkov, E.M. Dianov, GeO₂ influence on the formation of near-infrared emitting centers in Bi-doped multicomponent silicate glasses. Laser Phys. **24**(11), 115301 (2014)

25. N. Zhang, J.R. Qiu, G.P. Dong, Z.M. Yang, Q.Y. Zhang, M.Y. Peng, Broadband tunable near-infrared emission of Bi-doped composite germanosilicate glasses. J. Mater. Chem. **22**(7), 3154–3159 (2012)

26. T. Senden, F.T. Rabouw, A. Meijerink, Photonic effects on the radiative decay rate and luminescence quantum yield of doped nanocrystals. ACS Nano **9**(2), 1801–1808 (2015)

27. C. Xu, C.Y. Wang, J.D. Yu, R.L. Zhang, J.J. Ren, X.F. Liu, J.R. Qiu, Structure and optical properties of Er-doped CaO–Al₂O₃ (Ga₂O₃) glasses fabricated by aerodynamic levitation. J. Am. Ceram. Soc. **100**(7), 2852–2858 (2017)

28. M. Nouri, M. Tavoosi, P. Alizadeh, Processing and optical properties of transparent GeO₂–PbO–MgO–MgF₂ glass-ceramics. Ceram. Int. **42**(15), 17524–17529 (2016)

29. L.Y. Zhang, H. Li, L.L. Hu, Statistical structure analysis of GeO₂ modified Yb³⁺: phosphate glasses based on raman and FTIR study. J. Alloys Compd. **698**, 103–113 (2017)

30. A.M. Abdelghany, F.H. ElBatal, H.A. ElBatal, F.M. EzzElDin, Optical and FTIR structural studies of CoO-doped sodium borate, sodium silicate and sodium phosphate glasses and effects of gamma irradiation—a comparative study. J. Mol. Struct. **1074**, 503–510 (2014)

31. D. Dorosz, J. Zmojda, M. Kochanowicz, P. Miluski, P. Jelen, M. Sitarz, Structural and optical study on antimony-silicate glasses doped with thulium ions. Spectrochim. Acta A **134**, 608–613 (2015)

32. M.T. David, T. Antonella, S. Andrijana, L. Esposito, Effects of SiO₂ addition on TiO₂ crystal structure and photocatalytic activity. J. Eur. Ceram. Soc. **30**(12), 2481–2490 (2010)

33. J.A. Duffy, M.D. Ingram, Optical basicity-IV: influence of electronegativity on the Lewis basicity and solvent properties of molten oxyanion salts and glasses. J. Inorg. Nucl. Chem. **37**(5), 1203–1206 (1975)

34. J.A. Duffy, M.D. Ingram, An interpretation of glass chemistry in terms of the optical basicity concept. J. Noncryst. Solids **21**(3), 373–410 (1976)

35. A.A. Veber, A.N. Romanov, O.V. Usovich, Z.T. Fattakhova, E.V. Haula, V.N. Korchak, L.A. Trusov, P.E. Kazin, V.B. Sulimov, V.B. Tsvetkov, Luminescent properties of Bi-doped polycrystalline KAlCl₄. Appl. Phys. B **108**(4), 733–736 (2012)

36. Y.F. Xue, J.K. Cao, Z.Y. Zhang, L.P. Wang, S.H. Xu, M.Y. Peng, Manipulating Bi NIR emission by adjusting optical basicity, boron and aluminium coordination in borate laser glasses. J. Am. Ceram. Soc. **101**(2), 624–633 (2018)